

Experimental observation of the generation of cutoff solitons in a discrete LC nonlinear electrical line

K. Tse Ve Koon,^{1,*} P. Marquié,² and P. Tchofo Dinda³¹*Université de Lyon, CREATIS, CNRS UMR 5220, Inserm U1044, INSA-Lyon, Université Lyon 1, 69622 Villeurbanne Cedex, France*²*Laboratoire LEII, UMR CNRS No. 5158, Université de Bourgogne, B.P. 47870, 21078 Dijon, France*³*Laboratoire Interdisciplinaire Carnot de Bourgogne (ICB), UMR CNRS No. 6303, Université de Bourgogne, B.P. 47870, 21078 Dijon, France*

(Received 25 July 2014; published 3 November 2014)

We address the problem of supratransmission of waves in a discrete nonlinear system, driven at one end by a periodic excitation at a frequency lying above the phonon band edge. In an experimental electrical transmission line made of 200 inductance-capacitance LC cells, we establish the existence of a voltage threshold for a supratransmission enabling the generation and propagation of cut-off solitons within the line. The decisive role of modulational instability in the onset and development of the process of generation of cut-off solitons is clearly highlighted. The phenomenon of dissipation is identified as being particularly harmful for the soliton generation, but we show that its impact can be managed by a proper choice of the amplitude of the voltage excitation of the system.

DOI: [10.1103/PhysRevE.90.052901](https://doi.org/10.1103/PhysRevE.90.052901)

PACS number(s): 05.45.Yv, 42.65.Tg

I. INTRODUCTION

Energy transmission in a nonlinear medium by a periodic driven boundary whose period falls inside a forbidden band gap of the medium, has been shown to be a universal phenomenon called nonlinear supratransmission [1]. It has then been demonstrated to successfully apply to various physical systems, such as, Josephson junction parallel array [2], Bragg gap soliton generation, or to breather soliton generation in discrete nonlinear electrical lines [3]. This concept initially developed on one-dimensional systems has been successfully applied on two-dimensional systems [4,5]. In addition to the initial periodic driven boundary, various ways to achieve supratransmission have also been proposed [6–8].

One of the most useful results of the theory of nonlinear supratransmission is the demonstration of the existence of well-defined intensity thresholds above which transmission occurs. In many existing systems, the availability of explicit expressions for the threshold intensity allows one to tune the driving such as to work right below transmission, and thus design a device (detector or switch) that can respond to any weak superimposed signal, either by propagating solitons (or breathers) in the long-line case, or by bifurcating to an excited new state in the short-line case. The earlier studies on nonlinear supratransmission have been performed for systems with band-pass-type dispersion laws [1]. It was shown that when the external driving frequency is chosen inside the lower forbidden gap, the generated local excitations are called gap solitons. Later on, nonlinear supratransmission was shown to occur in discrete systems above the cut-off frequency [3,9]. Indeed it is an intrinsic property of a discrete system to possess a cut-off frequency in the dispersion curve, above which no propagation of a linear signal can occur. In Ref. [3] the authors examined the outstanding features of nonlinear supratransmission and bistability, above the cut-off frequency, in a short line made of 18 inductance-capacitance cells (LCs) submitted to a periodic voltage applied to the first cell.

Experimentally, they established the existence of a voltage threshold for the supratransmission enabling the generation and propagation of breather excitations within the line, and demonstrated the presence of the nonlinear bistability in this discrete system. On the other hand, by examining a long LC line consisting of 2000 cells, they demonstrated by numerical simulations that a periodic forcing slightly above the cut-off frequency, above a certain threshold of voltage amplitude, may generate cut-off solitons along the line.

In this work we examine a discrete LC nonlinear electrical line, and we achieve the experimental demonstration of the generation of the cut-off solitons predicted in Ref. [3]. We identify modulational instability as being the fundamental physical phenomenon that induces and governs the generation of the cut-off solitons. We show that the experimental line is prone to dissipation effects induced by the internal resistances of the inductances. We find that dissipation does not prevent the occurrence of the MI process, but affects strongly its development, and makes difficult the achievement of rigorous experimental measurements of the characteristics of the cut-off solitons.

II. SUPRATRANSMISSION THRESHOLD

The system under consideration is a discrete nonlinear LC line represented in Fig. 1. It is made of an array of elementary cells, each cell consisting of an inductance L , a nonlinear capacitor $C(V)$, and a resistance r to account for the dissipation induced by each inductance. The nonlinear element is a voltage-dependent capacitor, consisting of a BB112 reversed-biased diode. Following Ref. [10] the capacitance-voltage relationship can be expanded in Taylor series up to the second order, as follows:

$$C(\bar{V} + V_n) = C \times [1 - 2\alpha V_n + 3\beta V_n^2], \quad (1)$$

where \bar{V} is the dc bias voltage. As we shall operate around $\bar{V} = 2V$, with $|V_n| \leq 2V$, we have then:

$$C = 320 \text{ pF}, \quad L = 220 \text{ } \mu\text{H} \\ \alpha = 0.21 \text{ V}^{-1}, \quad \beta = 0.0197 \text{ V}^{-2}. \quad (2)$$

*kevin.tsevekoon@creatis.univ-lyon1.fr

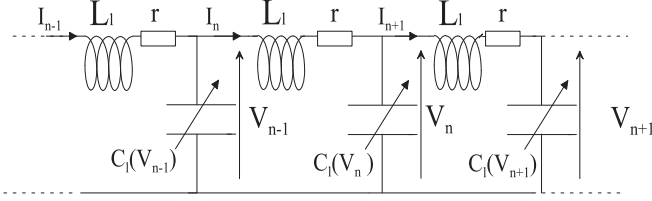


FIG. 1. Standard discrete nonlinear low-pass electrical line.

Applying Kirchoff's laws to this system leads to the following set of propagation equations:

$$\left\{ \frac{d^2}{dt^2} + \frac{r}{L} \frac{d}{dt} \right\} (V_n - \alpha V_n^2 + \beta V_n^3) = \frac{1}{LC} (V_{n+1} + V_{n-1} - 2V_n), \quad (3)$$

for $n = 1, 2, \dots, N$. The corresponding (linear) dispersion law of the plane-wave solution $\exp[i(kn - 2\pi ft)]$ is given by

$$f = f_c \sin(k/2), \quad f_c = \frac{1}{2\pi\sqrt{LC}}, \quad (4)$$

where f_c is the cut-off frequency for linear waves. This nonlinear system was shown [3] to exhibit supratransmission properties if it is harmonically forced at one end [$V_0(t) = \tilde{V}_0 \cos(\omega t)$ with $\omega > 2\pi f_c$] with an amplitude above a certain threshold ($\tilde{V}_0 > V_{th}$) given by:

$$V_{th} = 4\sqrt{\frac{\omega - \omega_c}{\omega_c(2\alpha^2 - 3\beta)}}. \quad (5)$$

In Ref. [3], it was shown that the application of a voltage excitation above the threshold V_{th} gives rise to an instability, which leads to the generation and propagation of cut-off solitons, and therefore, to energy transmission in the electrical line.

In this paper, we present the experimental evidence of this propagation of cut-off solitons. To this end, it is beforehand necessary to carry out numerical simulations in order to assess at best the experimental settings and the operational conditions. In this preliminary stage, it is worth noting that the above theoretical model contains some approximations as compared to the actual transmission line, which will need to be taken into consideration. In particular, it is worth noting that:

(i) The dissipation phenomenon, which is not taken into account in our model, will certainly perturb the supratransmission and the generation of cut-off solitons.

(ii) The system under consideration is a semi-infinite line, i.e., a line in which reflected waves and standing waves, cannot in principle be generated. However, in practice, it is impossible to construct a line really semi-infinite. Nevertheless, one may arrange so that the line be long enough to prevent the appearance of standing wave.

In the next section, we describe results of numerical simulations that we have carried out in the above-mentioned conditions.

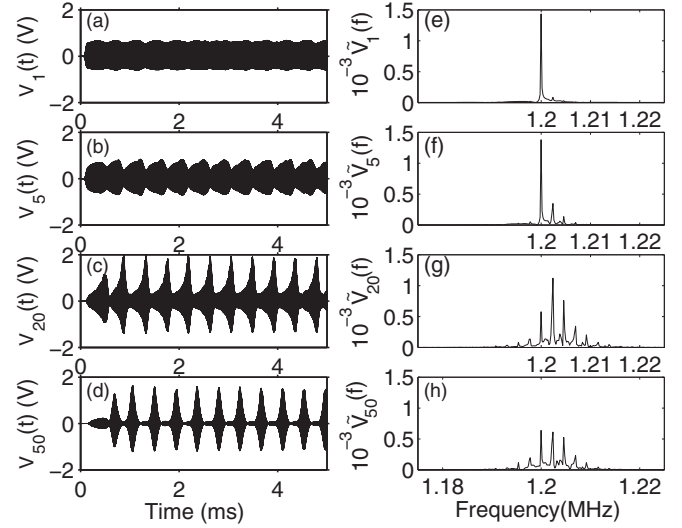


FIG. 2. Temporal variations of the voltage at cells number 1 (a), 5 (b), 20 (c), and 50 (d) and their respective spectra (e)–(h) obtained from numerical simulations on a 2000 cells electrical line with a driving amplitude of 0.6 V and a frequency of 1.2 MHz.

III. NUMERICAL SIMULATIONS

A. Generation process of cut-off solitons

We first have carried out numerical simulations of the nondissipative system, and have recorded the temporal dynamics of the voltage at four different sites of the line. Figure 2 shows typically the results obtained at cells number 1, 5, 20, and 50, with a driving amplitude of 0.6 V and a frequency of 1.2 MHz ($f_c = 1.197$ MHz).

Figures 2(a)–2(d) suggest that modulational instability (MI) is probably the precursor phenomenon of the formation of the soliton train, which begins to be clearly visible beyond the cell 50. Figures 2(e)–2(h), which show the spectra of the observed signals, tend to confirm the decisive role of the MI phenomenon. However, a careful inspection reveals a striking asymmetry in the spectra of the observed signals, which is unusual in ordinary MI spectra, in which sidebands are always generated symmetrically on each side of the driving frequency. Here, it is worth noting that in our system, the MI sidebands are preferentially generated in the (linear) forbidden band, at a modulation frequency f_m , which is found to be 2.3 kHz in the case of Fig. 2.

On the other hand, we have carried out additional numerical simulations for the same driving frequency (1.2 MHz) but with different driving amplitudes in the following range [0.4, 1.2]. At frequency of 1.2 MHz the amplitude threshold is equal to 0.38 V (giving the lower edge of our amplitude range), and for a driving amplitude of 1.2 V, the resulting solitons have an amplitude of the order of 2.5 V [which, by the way, is out of the limits of our model (1)].

If we assume that the MI frequency corresponds to the peak of MI gain then, according to Ref. [11], there should be a linear relationship between the wave vector δ corresponding to the MI frequency, and the driving amplitude:

$$\delta = A_0 \sqrt{\frac{Q}{P}}, \quad (6)$$

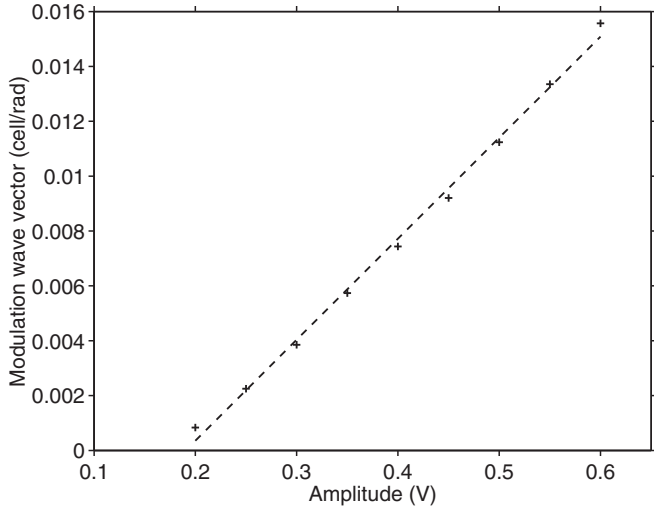


FIG. 3. Variation of the modulation wave vector with the amplitude for a driving frequency of 1.2 MHz.

where A_0 is the wave amplitude in the NLS approximation of the propagation equations (and is equal to half the driving amplitude), Q and P are the nonlinear and dispersion coefficients, respectively [3]. The wave vector δ is obtained by substituting the MI frequency f_m in the linear dispersion relationship [Eq. (4)]:

$$\delta = 2 \arcsin \left(\frac{f_m}{f_c} \right). \quad (7)$$

Figure 3 shows the variation of the wave vector δ as a function of the amplitude A_0 . As can be seen, the dependence of δ in respect to A_0 is essentially linear, in excellent agreement with Eq. (6). The linear fit (dashed line) gives us $\sqrt{\frac{Q}{P}} = 0.0368$.

We can thus conclude that modulational instability is the underlying process of the generation of cut-off solitons.

B. Dissipation effects

Dissipation is mainly due to the internal resistances of the inductances used in our experimental setup. It was demonstrated that [3] the main effects of dissipation on the supratransmission phenomenon is to increase the amplitude thresholds and to cause a kind of smoothing, i.e., a more progressive energy transmission. Although it was shown that the transmission of energy in this system (in the form of breather excitations) is possible in the presence of dissipation [3], one can however wonder whether the generation of cut-off solitons via a MI process will be also possible in the presence of a strong dissipation. Hence, before setting up our experiments, it is worth gaining an insight into the impact of dissipation on our system. But here, it is not possible to perform numerical simulations with exactly the same values of components as those available for our experiments. Indeed, because of dissipation, the voltage thresholds actually needed for the generation of cut-off solitons are higher than the threshold (of the nondissipative system) given in the formula (5). The larger the resistance r , the higher the real threshold is. According to

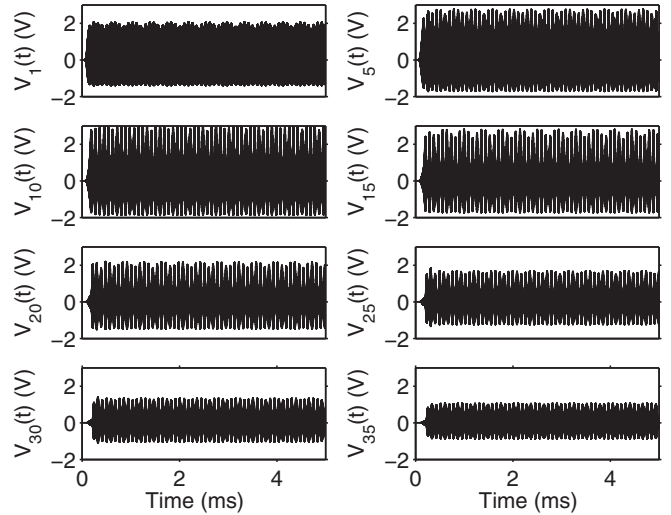


FIG. 4. Temporal evolutions at cells 1, 5, 10, 15, 20, 25, 30 and 35 obtained from numerical simulations with a driving amplitude of 1.5 V, frequency of 1.2 MHz and with a dissipation of $r = 5 \Omega$.

the data provided by the manufacturers of our components, in the experimental conditions that are envisaged (carrier frequency of 1.2 MHz, amplitude A_0 around 2V) the values of resistance r should fluctuate around a value of at least 20Ω . Now, we have found by simulations that in a line of 200 cells, such values of r lead to a dramatic increase of the voltage thresholds, well beyond [0.4, 1.2]. For example, a resistance of 10Ω causes the amplitude threshold to go up to 1.92 V (instead of 0.38 V in the nondissipative system). To obtain the main general features of the effects of dissipation without rescaling all component values of our theoretical model, we have carried out numerical simulations in the same conditions as those specified above but with a resistance value of 5Ω .

Figures 4 shows the temporal voltage evolution obtained at cells 1, 5, 10, 15, 20, 25, 30, and 35, for a driving frequency

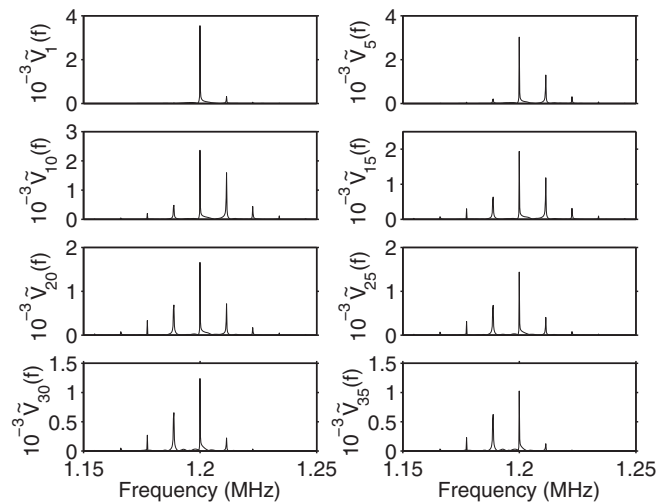


FIG. 5. Spectral evolutions at cells 1, 5, 10, 15, 20, 25, 30 and 35 obtained from numerical simulations with a driving amplitude of 1.5 V, frequency of 1.2 MHz and with a dissipation of $r = 5 \Omega$.

of 1.2 MHz and amplitude of 1.5 V while Fig. 5 illustrates the resulting spectra.

As can be seen, MI is quite present in spite of the presence of dissipation, but this instability does not develop until the formation of a well defined train of solitons.

On the other hand, in Fig. 5, we can observe that the amplitudes of the generated sidebands decrease as one moves away from the driven end of the line. Another noticeable difference concerns the position of the sidebands. Indeed, while in the nondissipative system the sidebands grow mostly inside the forbidden band (as Fig. 2 show), in presence of dissipation the development of the MI process becomes more elaborate. Hence, one can observe in the spectra of the dissipative system (Fig. 4) that in the first section of the line (between the first and the fifteenth cell), the wave dynamic is quite similar to that of the nondissipative system. This means that the effects of dissipation have not yet reached a level that is harmful for the process of generation of cut-off solitons. The MI phenomenon, which is the onset of the generation of solitons, is thus well created in the dissipative system, and generates the spectral components of the soliton around the carrier wave. The components generated in the lower side of the spectrum fall into the pass band and disperse, while the components of the top of the spectrum develop. From the entry of the line up to the surroundings of cell 15, the spectrum develops in an asymmetric way in each side of the carrier frequency (1.19 kHz). Beyond this region, the effects of dissipation begin to manifest themselves in a very harmful way, by causing a continual attenuation of the spectral components of the top side of the spectrum. At the same time, the components of the lower side of the spectrum, which initially were of dispersive nature, begin to grow.

Furthermore, we have measured the modulation frequency, which turns out to be 11.4 kHz and less than the value of 13.6 kHz obtained in the same conditions in the nondissipative system. We have also observed the above mentioned general features for resistance values of 1 and 10 Ω . More importantly, we have found for the dissipative system that the modulation

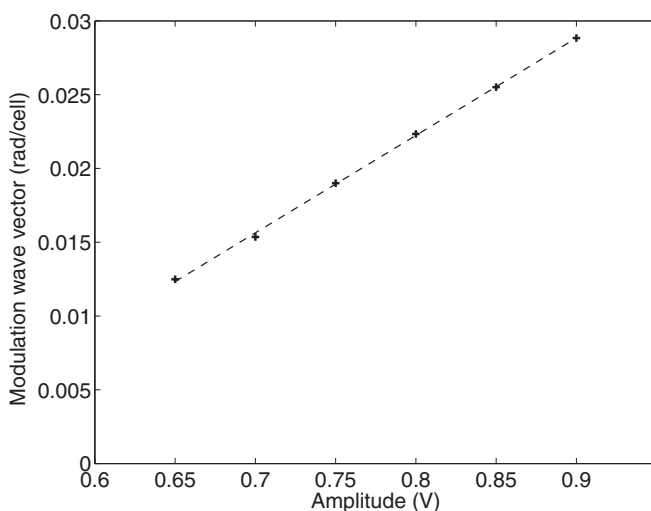


FIG. 6. Variation of the modulation wave vector with the amplitude for a driving frequency of 1.2 MHz in presence of dissipation; $r = 5\Omega$.

wave vector still varies linearly with the driving amplitude, as shown in Fig. 6, which confirms our prediction (already made for the nondissipative system) that MI is the underlying process that induce the generation of cut-off solitons. In the dissipative system, MI activates and develops this process of soliton generation, but this development is strongly hampered by the gradual attenuation of the spectral components of soliton, and the aforementioned instability of the global spectral structure of the system, where waves that were originally of dispersive nature become nondispersive during propagation, and vice versa.

IV. EXPERIMENTAL OBSERVATIONS

In our effort to observe the generation of cut-off solitons, we have built a line of 200 cells. This line is long enough to damp reflected waves and prevent stationary wave formation. Here, it is worth noting that the main virtue of our theoretical model (in Fig. 1), lies in its simplicity and its ability to clearly highlight the fundamental physical phenomenon that governs the generation of cut-off solitons, i.e., the MI. However this model provides only an idealized representation of certain characteristics of the real system, which can lead to quantitative differences between the theoretical predictions and experimental measurements. For example, in the theoretical model the values of the components are exactly the same in all cells. In reality, the values of the components always fluctuate around the value specified by the manufacturer. This fluctuation is of the order of 10% for the components used in our experimental setup, which would correspond to a fluctuation of the cut-off frequency between 1.14 MHz and 1.26 MHz. Nevertheless we have assumed that the effective cut-off frequency is equal to the theoretical one and have carried out measurements for frequencies ranging from 1.2–1.36 MHz.

A. Existence of a supratransmission threshold

Before examining the generation of solitons, it is important beforehand to demonstrate that our line has a supratransmission threshold. Hence, we have found that for a driving frequency of 1.2 MHz and amplitude of 4.94 V, the wave exhibits an evanescent profile. The amplitude of the voltage decreases abruptly, and then drops to a few millivolts as of the fifth cell. However, above this amplitude a sudden energy transmission occurs in the line and manifests itself by the presence of a relatively high level of voltage everywhere in the line but with an amplitude that decreases as one goes away from the entry of the line. Figures 7(a)–7(d) illustrate this supratransmission, in which the voltages are measured at cells 2, 10, 20, and 150 (using a four-channels Lecroy Waverunner oscilloscope) for a driving amplitude of 5 V.

We have carried out similar measures for frequencies ranging from 1.2–1.36 MHz, and obtained the results displayed in Fig. 8.

B. Cut-off soliton observation

We found that when the line is excited by voltages just above the supratransmission threshold, a MI phenomenon is well generated as illustrated clearly by the spectra of Figs. 7(e), 7(f), and 7(g), but this phenomenon does not continue until the formation of a train of solitons. The nongeneration of solitons

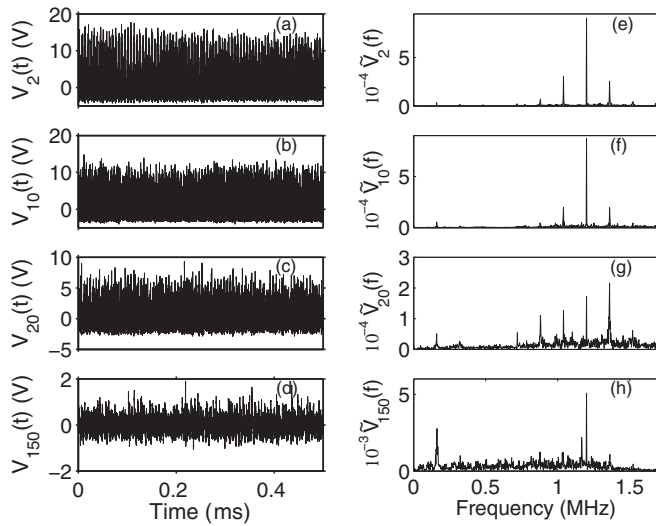


FIG. 7. (a)–(d) show experimental measures of the voltage obtained at cells 2, 10, 20, and 150 for a driving frequency of 1.2 MHz and frequency of 5 V while (e)–(h) show the corresponding spectrums.

is due to dissipation, which turns out be highly penalizing for such levels of amplitudes of excitation voltage. To reduce somewhat the impact of dissipation, we have used voltage levels clearly higher than the measured thresholds represented in Fig. 8. We have found that the resulting state of the electrical line submitted to such high amplitudes is unfortunately very unstable; which does not allow us to observe a steady regime with a single and well-defined train of cut-off solitons in motion. Among the various types of existing regimes, leading to more or less incoherent voltage profiles not represented here, we have succeeded in obtaining regimes where cut-off solitons are actually generated in our line. A typical example of such a soliton regime is represented in Figs. 9(a), 9(b), 9(c), and 9(d), where one can clearly observe that the modulation

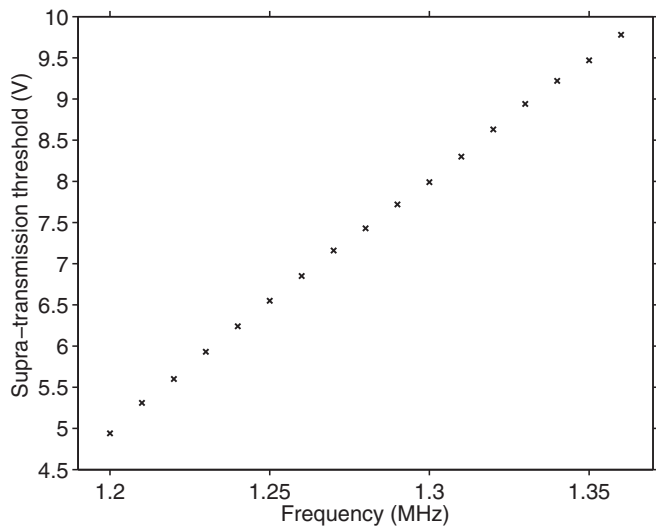


FIG. 8. Experimental supra-transmission threshold for driving frequencies varying from 1.2–1.36 MHz measured on a nonlinear LC electrical line.

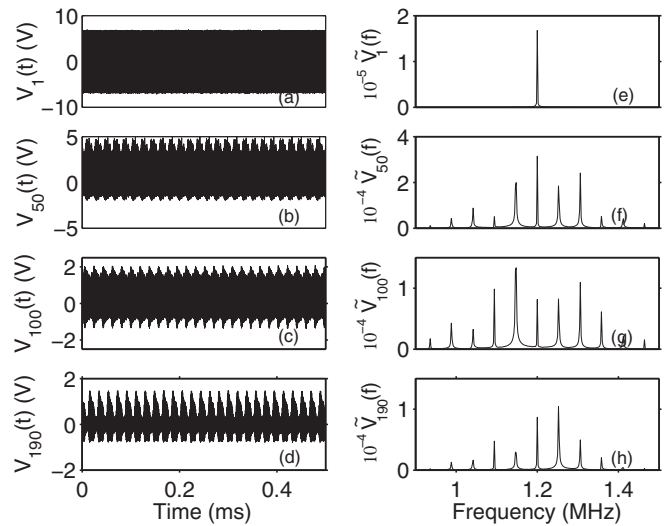


FIG. 9. (a)–(d) show experimental measurements of the voltage obtained at cells 1, 50, 100 and 190 for a driving frequency of 1.2 MHz and amplitude of 7 V while (e)–(h) show the corresponding spectra.

of the initial plane wave develops until the formation of pulses [visible in the Fig. 9(d)].

A careful inspection of Fig. 8(d) reveals that there is not only one but two soliton trains that are present in our line. The first one is the incident soliton train, which moves from the entry towards the free end of the line; while the second train corresponds to the solitons reflected at the free end of the line, which are moving in the opposite direction to that of the incident train, with amplitudes lowered by the dissipation. The presence of the two soliton trains is more clearly visible in Fig. 10, which is an enlargement of a portion of the voltage profile of Fig. 9(d). Note that we have performed numerical simulations (not shown here) on a lattice made of 200 cells with small dissipation and open end boundary conditions at the nondriven end. They have also revealed the presence of the two counterpropagating soliton trains observed experimentally.

We have verified that this regime, although not enough stable for permitting rigorous measurements, exists also at

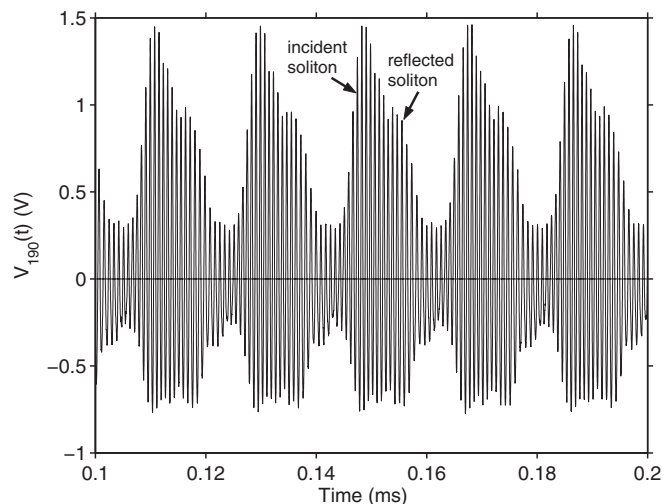


FIG. 10. Zoom of Fig. 9(d).

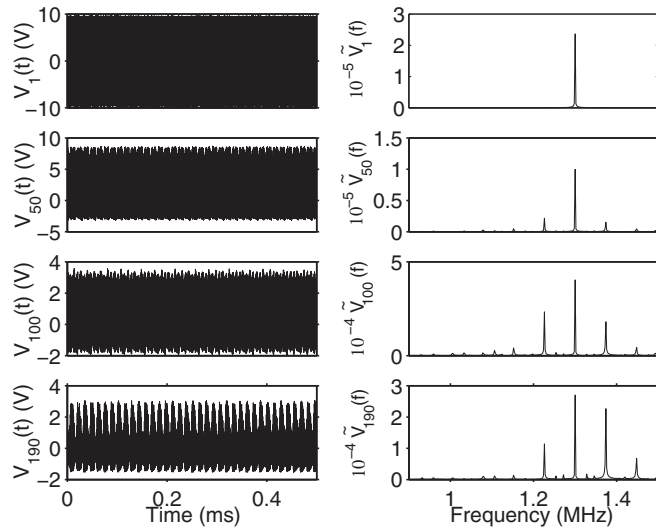


FIG. 11. Experimental measurements of the voltage and corresponding spectra obtained at cells 1,50,100, and 190 for a driving frequency of 1.3 MHz and amplitude of 9.9 V.

frequencies much higher than the cut-off frequency, as can be seen in Fig. 11, which show the results obtained for a driving frequency of 1.3 MHz, with a driving amplitude of 9.9 V (which is nearly the maximum amplitude delivered by our generator).

V. CONCLUSION

We have performed the first experimental observation of the generation and propagation of cut-off solitons on a 200-cell electrical line driven above its cut-off frequency. We have

shown that the process of generation of cut-off solitons is induced by a MI phenomenon, which is responsible for the creation and the development of the spectral components of the soliton. But we also observed that this generation of solitons is heavily hampered by the dissipation resulting from the imperfection of the components of the electric line (inductances). We have shown that dissipation does not prevent the occurrence of the MI process, but strongly affects its development and makes difficult any rigorous experimental measurement of the characteristics of the cut-off solitons.

In particular, we have shown that dissipation prevents the generation of solitons when the excitation voltages are close to the theoretical threshold of supratransmission in a model of nondissipative line. Solitons are generated for voltages significantly higher than the thresholds of supratransmission. In our experiments, it was not possible to generate a single train of solitons, but rather two trains of solitons propagating in opposite directions; an incident train and a reflected train.

It follows from our study that to generate a single and well-defined train of solitons in the experimental line, it is essential to use components of very high quality in terms of dissipation. Then, one can envisage either to lengthen the line sufficiently or to connect the free end of the line to its characteristic impedance.

But the most remarkable point of our study is the demonstration of a process of generation of cut-off solitons, by means of a relatively simple experimental setup containing only two types of components (inductance and capacitor).

ACKNOWLEDGMENT

The authors would like to acknowledge helpful discussion with their late colleague Jérôme Léon.

-
- [1] F. Geniet and J. Leon, *Phys. Rev. Lett.* **89**, 134102 (2002).
 - [2] D. Chevriaux, R. Khomeriki, and J. Leon, *Phys. Rev. B* **73**, 214516 (2006).
 - [3] K. Tse Ve Koon, J. Leon, P. Marquié, and P. Tchofo Dinda, *Phys. Rev. E* **75**, 066604 (2007).
 - [4] J. E. Macías-Díaz, *Phys. Rev. E* **77**, 016602 (2008).
 - [5] J. E. Macías-Díaz, *Phys. Rev. E* **78**, 056603 (2008).
 - [6] B. Bodo, S. Morfu, P. Marquié, and B. Z. Essimbi, *J. Stat. Mech.* (2009) P01026.
 - [7] G. Yu, X. Wang, and Z. Tao, *Phys. Rev. E* **83**, 026605 (2011).
 - [8] A. B. Togueu Motcheyo, C. Tchawoua, and J. D. Tchinnang Tchameu, *Phys. Rev. E* **88**, 040901(R) (2013).
 - [9] R. Khomeriki, S. Lepri, and S. Ruffo, *Phys. Rev. E* **70**, 066626 (2004).
 - [10] P. Marquié, J. M. Bilbault, and M. Remoissenet, *Phys. Rev. E* **49**, 828 (1994).
 - [11] T. B. Benjamin and J. E. Feir, *J. Fluid Mech.* **27**, 417 (1967).